



## OPEN

# The effect of doping Sb on the electronic structure and the device characteristics of Ovonic Threshold Switches based on Ge-Se

Sang-Yeol Shin<sup>1,2</sup>, J. M. Choi<sup>1</sup>, Juhee Seo<sup>1,3</sup>, Hyung-Woo Ahn<sup>1</sup>, Yong Gyu Choi<sup>2</sup>, Byung-ki Cheong<sup>1</sup> & Suyoun Lee<sup>1</sup>

<sup>1</sup>Electronic Materials Research Center, Korea Institute of Science and Technology, Hwarangno 14-gil 5, Seongbuk-gu, 136-791, Seoul, Republic of Korea, <sup>2</sup>Department of Materials Science and Engineering, Korea Aerospace University, Gyeonggi, 412-791, Republic of Korea, <sup>3</sup>Department of Nanomaterials Science and Engineering, University of Science and Technology, Daejeon 305-350, South Korea.

Received  
16 June 2014

Accepted  
29 October 2014

Published  
18 November 2014

Correspondence and requests for materials should be addressed to S.L. (slee\_eels@kist.re.kr)

The Ovonic Threshold Switch (OTS) based on an amorphous chalcogenide material has attracted much interest as a promising candidate for a high-performance thin-film switching device enabling 3D-stacking of memory devices. In this work, we studied on the electronic structure of amorphous Sb-doped  $\text{Ge}_{0.6}\text{Se}_{0.4}$  (in atomic mole fraction) film and its characteristics as to OTS devices. From the optical absorption spectroscopy measurement, the band gap ( $E_g$ ) was found to decrease with increasing Sb content. In addition, as Sb content increased, the activation energy ( $E_a$ ) for electrical conduction was found to decrease down to about one third of  $E_g$  from a half. As to the device characteristics, we found that the threshold switching voltage ( $V_{th}$ ) drastically decreased with the Sb content. These results, being accountable in terms of the changes in the bonding configuration of constituent atoms as well as in the electronic structure such as the energy gap and trap states, advance an effective method of compositional adjustment to modulate  $V_{th}$  of an OTS device for various applications.

Electronic switches including transistors and diodes are the most elementary building blocks of numerous electronic devices such as logic, memory, and display devices. As a result of incessant scale-down, switches based on single crystalline silicon are now considered to confront their limits in both performances and scalability. Scientists and engineers are struggling to find solutions which often exploit new materials, new device structures, and new operation principles. Among them, increasing attention has been paid to the Ovonic Threshold Switching (OTS) device owing to its high-current-driving capability and simple device structure<sup>1</sup>. S. R. Ovshinsky firstly reported reversible electrical switching phenomenon using a chalcogenide composed of Te, As, Si, and Ge in 1968, featured by a sudden huge drop in its resistance at a certain bias and the recovery of its initial high resistance state upon removal of the bias<sup>2,3</sup>. About 40 years after the discovery, a successful integration into a phase-change memory was demonstrated and a switching speed being as fast as several nsec was also shown promising<sup>4,5</sup>. However, there still exist a few issues to deal with for achieving a reliable OTS device. For one issue, most of the chalcogenide materials used in the OTS device consist of environment-unfriendly compounds containing As. To resolve this issue, we investigated the feasibility of more environment-friendly and simple binary chalcogenide materials,  $\text{Ge}_x\text{Se}_{1-x}$  ( $x = 0.4\sim 0.7$ ), and demonstrated their reliable characteristics as materials for OTS devices<sup>6</sup>. As another issue, one should be able to tailor the operational characteristics of such OTS in effective and controllable manners for these devices to be integrated in various functional devices. For that matter, threshold switching voltage ( $V_{th}$ ), a fundamental parameter characterizing an OTS, is to be singled out. According to a recent model developed by D. Ielmini,  $V_{th}$  depends on the energy gap ( $E_g$ ), the density ( $n_{trap}$ ) and the energy level ( $E_{trap}$ ) of trap states<sup>7,8</sup>. Doping of group-V elements as well as varying the kind of chalcogen atoms (S, Se, Te) could modify the electronic structure of the amorphous chalcogenide with concomitant modulation of the switching characteristics, as shown with N- and Bi-doped  $\text{Ge}_{0.6}\text{Se}_{0.4}$  systems<sup>9,10</sup>. Herein, we have extended the approach to Sb and systematically studied the effect of its doping in  $\text{Ge}_{0.6}\text{Se}_{0.4}$  on the electronic structures and

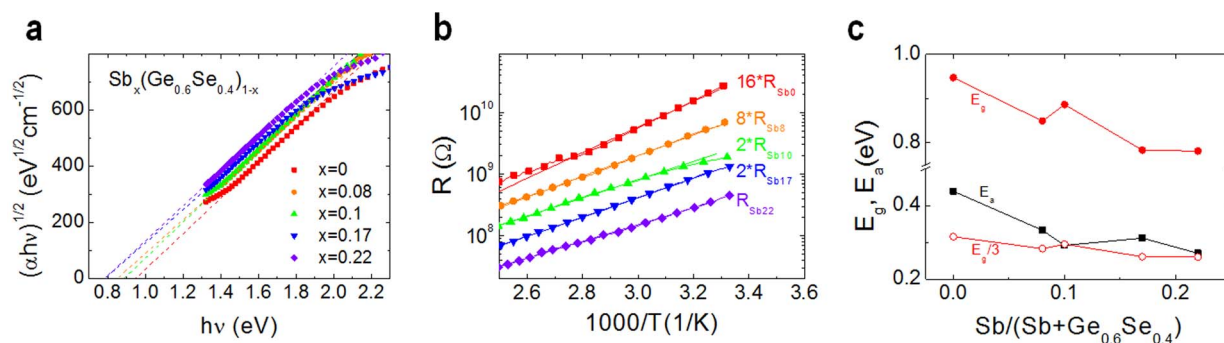


**Figure 1** | (a) Tauc plot ( $(\alpha hv)^{1/2}$  vs.  $h\nu$ ) of  $\text{Sb}_x(\text{Ge}_{0.6}\text{Se}_{0.4})_{1-x}$  films. The dashed lines are the linear fits to the data. (b) Semilog-plot of the resistance ( $R$ ) of the  $\text{Sb}_x(\text{Ge}_{0.6}\text{Se}_{0.4})_{1-x}$  films as a function of the reciprocal of the temperature ( $T$ ) (Arrhenius plot). The solid lines are the linear fits to the data. The curves are vertically shifted for clarity (multiplication factors are indicated on the left of the curve). (c) The energy gap ( $E_g$ ; solid red circle) and the activation energy for electrical conduction ( $E_a$ ; solid black square) as a function of Sb contents.  $E_g/3$  is also plotted for comparison with  $E_a$ .

the characteristics of OTS devices. In the previous reports<sup>11–13</sup>, Sb was shown to result in the reduction of  $E_g$  when doped in various amorphous  $\text{Ge}_x\text{Se}_y$  materials.

## Results and Discussion

Figure 1(a) shows the results of the optical absorption spectroscopy measurements for various  $\text{Sb}_x(\text{Ge}_{0.6}\text{Se}_{0.4})_{1-x}$  films. In many amorphous semiconductors, the dependence of the absorption coefficient ( $\alpha$ ) on the photon energy ( $h\nu$ ) is well expressed by Tauc's relation,  $\alpha hv \propto (h\nu - E_g)^2$  for  $h\nu > E_g$ , with a broad tail structure due to trap states for  $h\nu < E_g$ <sup>14</sup>. In Figure 1(a), it is found that  $\sqrt{\alpha hv}$  depends linearly on  $h\nu$  for each film in the high photon energy regions. From the slope of each curve,  $E_g$  of a respective film was obtained and the resultant  $E_g$  values are plotted as a function of Sb content in Figure 1(c). It is apparent that  $E_g$  decreases with increasing Sb content.

In Figure 1(b), we plotted the electrical resistance ( $R$ ) as a function of the reciprocal temperature ( $1/T$ ) for each film.  $T$  was increased from room temperature to  $420^\circ\text{C}$  at a rate of  $5^\circ\text{C}/\text{min}$ . For all the samples, variation in resistance with temperature was found to be well described by Arrhenius' law ( $R = R_0 \exp(E_a/kT)$ ), where  $E_a$  and  $k$  are the activation energy for the electrical conduction and Boltzmann constant, respectively. It should be mentioned that the observed data were also attempted to fit to the variable-range hopping model with an  $R \sim \exp[(T_0/T)^{1/4}]$  dependence but in vain (see Supplementary Information, Figure S1). In Figure 1(b), linear fitting curves are also shown (solid lines) while their slopes representing  $E_a$ 's of the films. Interestingly,  $E_a$  was found to approach  $E_g/3$  with increasing Sb content from  $E_g/2$  in the Sb-free case as shown in Figure 1(c). In most of the amorphous chalcogenide materials examined,  $E_a$  was usually found to be about one half of  $E_g$  and this was understood as resulting from the Fermi level pinning at the midgap due to a huge amount of charged defect centers<sup>13</sup>. Such a relationship ( $E_a \sim E_g/3$ ) was originally observed in  $\text{Bi}_x\text{Ge}_{0.2}\text{Se}_{0.8-x}$  and interpreted in terms of the incorporation of positively charged impurities<sup>16</sup>. In addition, such a relationship was found in recent studies on  $\text{Ge}_{0.4}\text{Te}_{0.6-x}\text{Sb}_x$ <sup>17</sup> and  $\text{Bi}_x(\text{Ge}_{0.5}\text{Se}_{0.5})_{1-x}$ <sup>10</sup>. Considering the electronegativity of Sb ( $\chi_{\text{Sb}} = 2.05$  eV) not much different from that of Bi ( $\chi_{\text{Bi}} = 2.02$  eV), but much lower than that of Se ( $\chi_{\text{Se}} = 2.55$  eV), the amount of positively charged impurities is expected to be similarly large in  $\text{Sb}_x(\text{Ge}_{0.6}\text{Se}_{0.4})_{1-x}$  with a high  $x$ , leading to the observation.

Meanwhile, the crystallization temperature ( $T_x$ ) values can be also determined from the measured  $R$  vs.  $T$  curves as  $R$  decreases drastically upon crystallization (see Figure S2 in Supplementary Information).  $T_x$  was found to decrease with increasing Sb content but was higher than  $350^\circ\text{C}$  even at the highest Sb content tested i.e.  $x = 0.22$ . This guarantees that the Sb-doped GeSe is not liable to

crystallize during device fabrication around at  $350^\circ\text{C}$ , a prerequisite for a material to be adopted in the OTS.

Figure 2(a) and 2(b) show schematic illustrations of an OTS device using  $\text{Sb}_x(\text{Ge}_{0.6}\text{Se}_{0.4})_{1-x}$  and of the electrical measurement setup for device characterization, respectively. To find  $V_{\text{th}}$  of each device, triangular voltage pulses were applied instead of DC voltage which forces enormous thermal and electrical stresses resulting in irreversible changes in device characteristics. A pulse composed of 1  $\mu\text{s}$  (rising time), 100 nsec (width), and 1  $\mu\text{s}$  (falling time) was applied while both the voltage across and the current through the device were measured with two oscilloscopes, OSC1 and OSC2, respectively. The size of a sample was varied from  $2 \times 2 \mu\text{m}^2$  to  $20 \times 20 \mu\text{m}^2$  and the data presented in this paper were obtained with devices of  $5 \times 5 \mu\text{m}^2$  in size. Figure 2(c) shows typical current ( $I$ ) – voltage ( $V$ ) curves of OTS devices of each composition.  $V_{\text{th}}$  is defined as the voltage at which a drastic change in device resistance comes about, initiating a snap-back in the  $I$ – $V$  curve. In Figure 2(d),  $V_{\text{th}}$  is shown to decrease remarkably as Sb content increases. The observed reduction in  $V_{\text{th}}$  agrees qualitatively with the reduction of  $E_g$ , which is expected from the aforementioned Ielmini's model<sup>7,8</sup>. But quantitatively, such a remarkable reduction of  $V_{\text{th}}$  by about 33.3% (from 3.24 V to 2.16 V as Sb content increases from 0 to 22 at. %) may not be solely ascribed to the reduction of  $E_g$  by about 17% ( $E_g = 0.94$  and 0.78 eV for  $\text{Ge}_{0.6}\text{Se}_{0.4}$  and  $\text{Sb}_{0.22}(\text{Ge}_{0.6}\text{Se}_{0.4})_{0.78}$ , respectively). According to our calculation using the Ielmini's model (See Figure S3 in Supplementary Information),  $V_{\text{th}}$  was shown to linearly depend on  $E_g$  with a slope of about one. Apart from  $E_g$ , two material parameters have significant effects on the characteristics of an OTS device. One is the density of trap states ( $n_{\text{T}}$ ) and the other is the energy difference ( $\Delta E$ ) between the trap level and the edge of the neighboring extended band (either valence band (VB) or conduction band (CB)). In our previous work<sup>18</sup>, we derived an expression describing the dependence of the delay time ( $t_{\text{del}}$ ) of an OTS on the bias voltage based on a simplified model assuming thermally-activated hopping transport and trap states of a single kind, from which  $n_{\text{T}}$  and  $\Delta E$  can be estimated. In Figure 3(a), a set of panels is shown with each representing a contour map of the current waveforms at varying  $V_a$  values, flowing through a typical OTS device of the respective film composition. The color scale represents the current levels measured with OSC2 shown in Figure 2(b). For these measurements, we applied a 200 ns-long voltage pulse of varying amplitude while registering the applied voltage ( $V_a$ ) with OSC1 and the current flowing through the device with OSC2. A representative waveform at  $V_a = 3.68$  V is shown in the inset for an undoped sample (leftmost panel). The black dashed lines indicate the beginning of the applied voltage pulse. It is apparent that  $V_{\text{th}}$  decreases as Sb content increases, consistent with Figure 2(c). Furthermore, it is observed that a threshold switching event

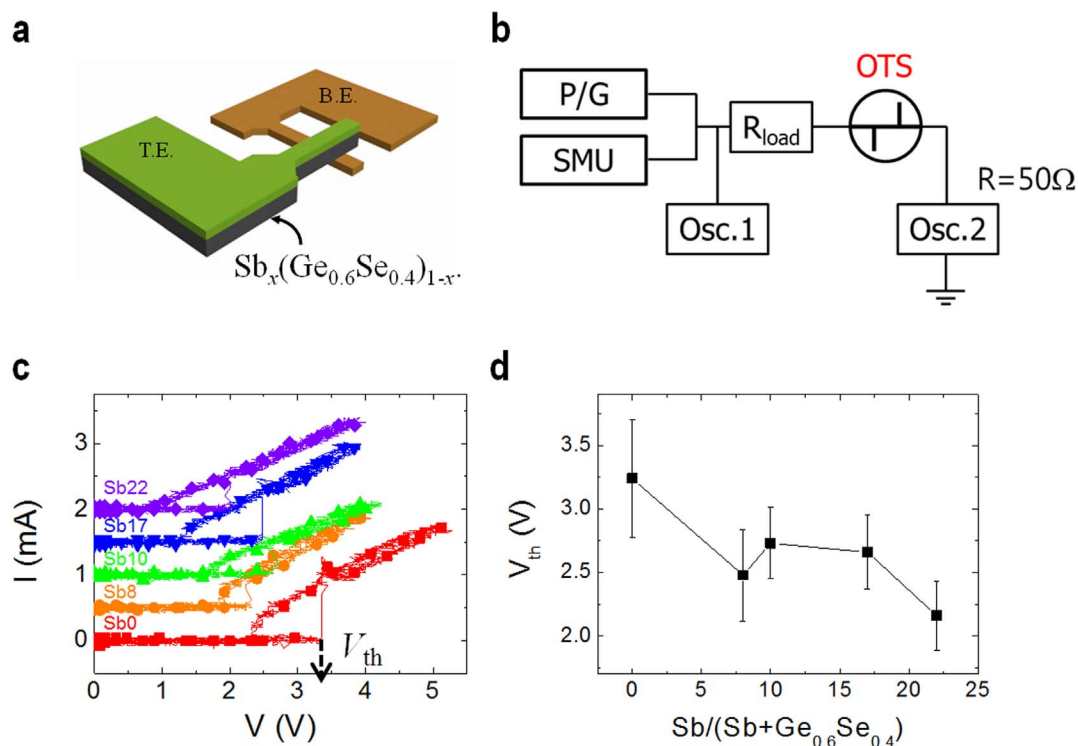


**Figure 2** | (a) and (b) Schematic illustrations of a cross-point OTS device and the measurement setup. (P/G: pulse generator, SMU: source-measure unit,  $R_{load}$ : load resistor). (c) Characteristic current ( $I$ )-voltage ( $V$ ) curves for typical OTS devices using  $Sb_x(Ge_{0.6}Se_{0.4})_{1-x}$ . It was measured by applying a 2  $\mu$ s-long triangular pulse and recording the voltage- and current-pulse waveforms by osc1 and osc2, respectively. The curves are vertically shifted in the order of Sb contents. (d) The dependence of  $V_{th}$  on the Sb contents, where  $V_{th}$  is defined in (c).

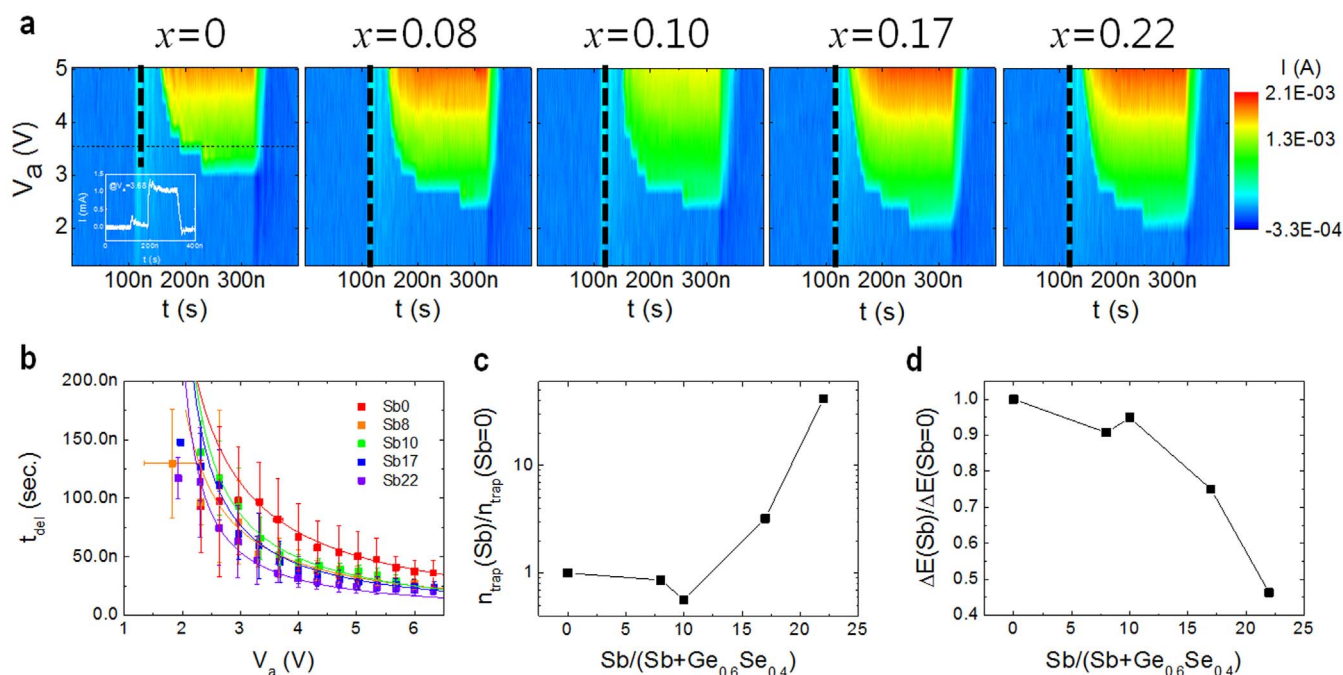


**Figure 3** | (a) Contour maps of current waveforms recorded in osc. 2 (in figure 2(b)) with varying  $x$ . Color scale represents the amplitude of current. 200 ns-long rectangular pulses were applied with increasing amplitude and the beginning of the voltage pulse is indicated by the dashed lines. For  $x = 0$  case, a current waveform at  $V_a = 3.68$  V is displayed in the inset. (b) The symbols represent  $t_{del}$  as a function of  $V_a$  for each composition. The solid lines are fitting curves by Eq. (1) in the text. Error bars means the standard deviation. (c) and (d)  $n_{trap}$  and  $\Delta E (= E_C - E_T)$  normalized by that of the  $x = 0$  sample as a function of Sb contents, respectively.



occurs at  $t_{\text{del}}$  after the voltage pulse is applied and that  $t_{\text{del}}$  decreases with increasing  $V_a$ . In ref. 18, the dependence of  $t_{\text{del}}$  on the bias voltage was shown to have the following expression.

$$t_{\text{del}} = \tau_0 \frac{\exp\left[\frac{1}{kT} \left\{ (E_c - E_T) - \frac{1}{2} q^* V_a \right\}\right] - \exp\left[-\frac{q^*}{kT} \left(\frac{3}{2} V_a - V_{\text{th}}\right)\right]}{1 - \exp\left[-\frac{1}{kT} q^* (V_a - V_{\text{th}})\right]} \quad (1)$$

In Eq. (1),  $\tau_0$ ,  $E_c$ ,  $E_T$ ,  $V_a$ , and  $k$  are the escape-trial time, conduction band minimum, energy level of trap states, applied voltage, and the Boltzmann constant, respectively. And  $q^*$  is the effective charge defined by  $e\Delta z/u_a$ , where  $\Delta z$  and  $u_a$  are the inter-trap distance and the thickness of the amorphous chalcogenides layer, respectively. In Figure 3(b), the curves of measured  $t_{\text{del}}(V_a)$  values are shown for OTS devices with  $\text{Sb}_x(\text{Ge}_{0.6}\text{Se}_{0.4})_{1-x}$  together with the fitting curves due to Eq. (1), where a data point with an error bar represents an average and a standard deviation taken over about 20 measurements using more than five devices. It is clear that, at low  $V_a$  region, the rate of change in  $t_{\text{del}}$  with  $V_a$  gets larger as Sb content increases. Conceivably, this is associated with the increase of the trap density ( $n_{\text{trap}}$ ) with Sb content. With increasing trap density, traps come closer to each other and the barrier height between them gets lower due to the Poole-Frenkel mechanism<sup>19</sup>. Such lowering of the barrier height leads to an exponential decrease in the escape-time from a trap hence in  $t_{\text{del}}$ . The calculated  $n_{\text{trap}}$  and  $\Delta E$  values are plotted in Figure 3(c) and 3(d), respectively. In Figure 3(c), the  $n_{\text{trap}}$  is found to increase as Sb content increases, consistent with the above explanation. In Figure 3(d),  $\Delta E$  is shown to decrease as Sb content increases, indicating that the trap states come closer to VB or CB.

The observed variations in  $n_{\text{trap}}$  and  $\Delta E$  are thought to be associated with the change in the electronic structure accompanying the one in bond configuration by Sb-doping in  $\text{Ge}_{0.6}\text{Se}_{0.4}$ . In amorphous materials, the atomic structure is determined by the average coordination number ( $\bar{C}$ ) given by the average of the coordination numbers of constituent atomic species weighted by the respective composition of each species. In our  $\text{Sb}_x(\text{Ge}_{0.6}\text{Se}_{0.4})_{1-x}$  system,  $\bar{C}$  ranges from 2.8 (for  $x = 0$ ) to 3.156 (for  $x = 0.22$ ), which are higher than Tanaka's threshold ( $\bar{C} = 2.67$ )<sup>20</sup>, indicating that the investigated materials in this work have 3D-network structures. The bond configurations constituting 3D-network structures may be conjectured according to the chemical ordered network model (CONM) proposed by Bicerano and Ovshinsky<sup>21</sup>. For this purpose, the bonding energies between constituent atoms should be known and they were calculated by using Pauling's relation in a previous paper as listed in Table 1<sup>22</sup>. From the listed bonding energies, the followings may be inferred as to bonding configurations. Firstly, the higher bonding energy of a Ge-Se pair than those of the other pairs i.e. Ge-Ge and Se-Se would lead to the preferential formation of  $\text{Ge}(\text{Se}_{1/2})_4$  tetrahedron in Ge-Se binary materials. Secondly, in the particular case of  $\text{Ge}_{0.6}\text{Se}_{0.4}$  material characterized by a relative Se-deficient composition, all Se atoms are bonded with Ge atoms to form  $\text{Ge}(\text{Se}_{1/2})_4$  tetrahedra and the remaining Ge atoms form homopolar Ge-Ge bonds. When Sb atoms are incorporated in  $\text{Ge}_{0.6}\text{Se}_{0.4}$ ,  $\text{Ge}(\text{Se}_{1/2})_4$  remain intact because of the highest bonding energy whereas a portion of Ge homopolar bonds would be replaced with Ge-Sb bonds

**Table 1 | Energy of possible bonds in  $\text{Ge}_x\text{Se}_y\text{Sb}_z$  compounds**

Bonds	Energy (kcal/mol)
Ge-Se	49.42
Sb-Se	43.96
Se-Se	44.00
Ge-Ge	37.60
Ge-Sb	33.76
Sb-Sb	30.22

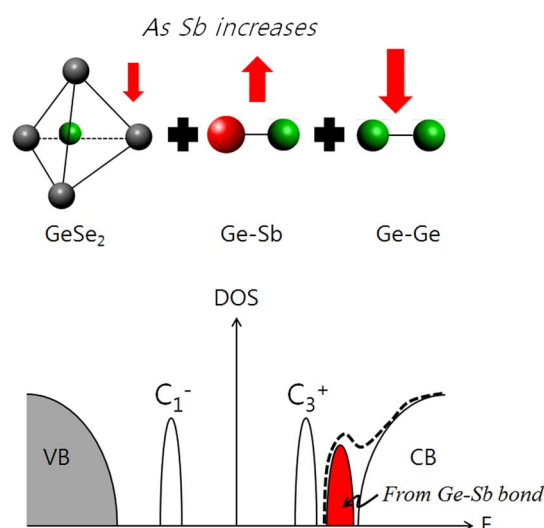


**Figure 4 | Schematic illustration of the change in bond configuration and the electronic structure by doping Sb in  $\text{Ge}_{0.6}\text{Se}_{0.4}$ .**

instead because of the preference of the heteropolar bonds to the homopolar bonds.

This change in bond configuration can result in significant changes in the electronic structure. The suggested change is schematized in Figure 4. In amorphous chalcogenides, it is assumed that a chalcogen atom has a two-fold coordination with its neighbors and the lone-pair (LP) electrons are configured spontaneously to form valence-alternation pairs (VAPs)<sup>3,23</sup>. VAPs are composed of two oppositely charged chalcogen atoms, leading respectively to donor-like trap ( $C_3^+$ ) and acceptor-like traps ( $C_1^-$ ) inside the band gap. We assume that this electronic structure may apply essentially to undoped amorphous  $\text{Ge}_{0.6}\text{Se}_{0.4}$ . For Sb-doped  $\text{Ge}_{0.6}\text{Se}_{0.4}$ , it should be noted that the preferred bond between Ge and Sb has the bonding energy lower than Ge homopolar bonds by about 3.9 kcal/mol. Weak bonds are expected to create localized anti-bonding states in the band gap leading to the Mott delocalization<sup>23</sup>. In addition, since an Sb atom has one more electron than a Ge atom, an Sb atom is expected to be ionized on forming a bond with Ge. These positively-charged impurities might create extra defect states broadening the trap states near CB. In this picture, it should be addressed that the assumed coordination number of an Sb atom is larger than the expected (=3) from the “8-N” rule, where N represents the number of valence electrons of a constituent atomic species (5 for Sb). The existence of over-coordinated Sb atoms is supported by a previous EXAFS study<sup>24</sup> and a density functional calculations<sup>25</sup>, where the coordination number of Sb in  $\text{Ge}_2\text{Sb}_2\text{Te}_5$  was found to be higher than three. This model can naturally explain the above observations and the resultant drastic reduction of  $V_{\text{th}}$  by Sb-doping.

In Figure S4, we plotted the off-state resistance ( $R_{\text{off}}$ ), the on-state resistance ( $R_{\text{on}}$ ), and the ratio between them ( $R_{\text{off}}/R_{\text{on}}$ ) as a function of Sb contents.  $R_{\text{off}}$  was measured by biasing DC 0.2 V and ( $R_{\text{on}}$ ) was measured by dividing the voltage amplitude of an applied pulse (200 ns-long) by the current amplitude. For  $x \leq 0.10$ ,  $R_{\text{off}}/R_{\text{on}}$  is found to be higher than  $10^5$ .

Considering that  $V_{\text{th}}$  changed mainly in the range of  $0 < x < 0.1$  (see Figure 2(d)), this work is believed to provide not only a method to modulate the threshold voltage of an OTS device for various applications by doping group-V elements, but also a promising candidate chalcogenide material to be employed for the development of a high-performance switching device beyond the Si era.

## Methods

$\text{Sb}_x(\text{Ge}_{0.6}\text{Se}_{0.4})_{1-x}$  thin films were fabricated by co-sputtering technique using Sb, Ge, and  $\text{Ge}_{0.4}\text{Se}_{0.6}$  targets, while the film composition was varied with changing RF



(radio-frequency) power imposed on each target. The Sb contents were determined to be 0, 8.3, 10.4, 17.4 and 22.5 at. % respectively by Electron Probe Micro Analysis (EPMA) and X-Ray Fluorescence (XRF) analysis. UV/VIS spectroscopy was performed with a 100 nm-thick film deposited on a corning glass substrate ( $t = 0.5$  mm) in the wavelength range of 300–1600 nm using UV/VIS/NIR spectrometer (UV 3600, Shimadzu). The electrical resistance ( $R$ ) was also measured as a function of temperature ( $T$ ) under the Ar atmosphere of 1 Torr using a standard four-point probe method. From the resulting  $R$  vs.  $T$  plot the activation energy ( $E_a$ ) for electrical conduction as well as the crystallization temperature ( $T_c$ ) was determined for each composition. The former is known to be related to  $E_g$  in amorphous chalcogenide due to the pinning of the Fermi level. The latter sets a limit in thermal loading below which the local structure of the used amorphous chalcogenide material can be secured. OTS devices were fabricated with each device having a cross-point structure composed of metal(bottom electrode, Pt 50 nm)/Sb<sub>x</sub>(Ge<sub>0.6</sub>Se<sub>0.4</sub>)<sub>1-x</sub>(100 nm)/metal(top electrode, TiN 50 nm) using photolithography and lift-off techniques. The size of a cross-point device was defined with the overlapping area of the top and bottom electrode metals. The device characteristics were investigated using a measurement setup composed of a source-measurement unit (Keithley 236), a multi-channel oscilloscope (Tektronix TDS 5104), and a pulse generator (agilent 81110A) (Figure 2(b)).

1. ITRS 2011 edition, Emerging Research Devices. Web-Site: <http://www.itrs.net/Links/2011ITRS/2011Chapters/2011ERD.pdf> (2011).
2. Ovshinsky, S. R. Reversible Electrical Switching Phenomena in Disordered Structures. *Phys. Rev. Lett.* **21**, 1450–1453 (1968).
3. Adler, D., Henisch, H. K. & Mott, S. N. The mechanism of threshold switching in amorphous alloys. *Rev. Mod. Phys.* **50**, 209–220 (1978).
4. DerChang, K. *et al.* A stackable cross point Phase Change Memory. *Electron Devices Meeting (IEDM) Baltimore, MD*, doi:10.1109/IEDM.2009.5424263 (2009, Dec. 7–9).
5. Anbarasu, M., Wimmer, M., Bruns, G., Salinga, M. & Wuttig, M. Nanosecond threshold switching of GeTe<sub>6</sub> cells and their potential as selector devices. *Appl. Phys. Lett.* **100**, 143505, doi:10.1063/1.3700743 (2012).
6. Kim, S.-D. *et al.* Effect of Ge Concentration in Ge<sub>x</sub>Se<sub>1-x</sub> Chalcogenide Glass on the Electronic Structures and the Characteristics of Ovonic Threshold Switching (OTS) Devices. *ECS Solid State Letters* **2**, Q75–Q77, doi:10.1149/2.001310ssl (2013).
7. Ielmini, D. Threshold switching mechanism by high-field energy gain in the hopping transport of chalcogenide glasses. *Phys. Rev. B* **78**, 035308 (2008).
8. Ielmini, D. & Zhang, Y. Analytical model for subthreshold conduction and threshold switching in chalcogenide-based memory devices. *J. Appl. Phys.* **102**, 054517, doi:10.1063/1.2773688 (2007).
9. Ahn, H.-W. *et al.* Effect of density of localized states on the ovonic threshold switching characteristics of the amorphous GeSe films. *Appl. Phys. Lett.* **103**, 042908, doi:10.1063/1.4816349 (2013).
10. Seo, J., Ahn, H.-W., Shin, S.-y., Cheong, B.-k. & Lee, S. Anomalous reduction of the switching voltage of Bi-doped Ge<sub>0.5</sub>Se<sub>0.5</sub> ovonic threshold switching devices. *Appl. Phys. Lett.* **104**, 153503, doi:10.1063/1.4871385 (2014).
11. Tichá, H. & Frumar, M. Optical absorption of glassy semiconductors of the Ge-Sb-Se system. *J. Non-Cryst. Solids* **16**, 110–116, doi:10.1016/0022-3093(74)90073-8 (1974).
12. Klocek, P. & Colombo, L. Index of refraction, dispersion, bandgap and light scattering in GeSe and GeSbSe glasses. *J. Non-Cryst. Solids* **93**, 1–16, doi:10.1016/S0022-3093(87)80023-6 (1987).
13. Abdel-Rahim, M. A., Moharram, A. H., Dongol, M. & Hafiz, M. M. Experimental studies of the Ge-Sb-Se system. *J. Phys. Chem. Solids* **51**, 355–359, doi:10.1016/0022-3697(90)90119-Z (1990).
14. Tauc, J., Grigorovici, R. & Vancu, A. Optical Properties and Electronic Structure of Amorphous Germanium. *Phys. Status Solidi B* **15**, 627–637, doi:10.1002/pssb.19660150224 (1966).
15. Tohge, N., Minami, T. & Tanaka, M. Preparation and conduction mechanism of n-type semiconducting chalcogenide glasses chemically modified by bismuth.

- J. Non-Cryst. Solids* **38–39**, Part 1, 283–288, doi:10.1016/0022-3093(80)90432-9 (1980).
16. Elliott, S. R. & Steel, A. T. Mechanism for Doping in Bi Chalcogenide Glasses. *Phys. Rev. Lett.* **57**, 1316–1319 (1986).
  17. Shukla, S. & Kumar, S. Electrical transport in thin films of glassy Ge<sub>40</sub>Te<sub>60-x</sub>Sb<sub>x</sub> alloys. *Semicond. Phys. Quantum Electron. Optoelectron.* **13**, 422–425 (2010).
  18. Lee, S. *et al.* A study on the temperature dependence of the threshold switching characteristics of Ge<sub>2</sub>Sb<sub>2</sub>Te<sub>5</sub>. *Appl. Phys. Lett.* **96**, 023501, doi:10.1063/1.3275756 (2010).
  19. Sze, S. M. *Physics of Semiconductor Devices* 3rd edition, Ch. 4 Silicon MOS capacitor [233–235] (Wiley, 2007).
  20. Tanaka, K. Structural phase transitions in chalcogenide glasses. *Phys. Rev. B* **39**, 1270–1279 (1989).
  21. Bicerano, J. & Ovshinsky, S. R. Chemical bond approach to the structures of chalcogenide glasses with reversible switching properties. *J. Non-Cryst. Solids* **74**, 75–84, doi:10.1016/0022-3093(85)90402-8 (1985).
  22. Sharda, S., Sharma, N., Sharma, P. & Sharma, V. Finger prints of chemical bonds in Sb–Se–Ge and Sb–Se–Ge–In glasses: A Far-IR study. *J. Non-Cryst. Solids* **362**, 136–139, doi:10.1016/j.jnoncrysol.2012.10.035 (2013).
  23. Kastner, M. Bonding Bands, Lone-Pair Bands, and Impurity States in Chalcogenide Semiconductors. *Phys. Rev. Lett.* **28**, 355–357 (1972).
  24. Paesler, M. A., Baker, D. A., Lucovsky, G., Edwards, A. E. & Taylor, P. C. EXAFS study of local order in the amorphous chalcogenide semiconductor Ge<sub>2</sub>Sb<sub>2</sub>Te<sub>5</sub>. *J. Phys. Chem. Solids* **68**, 873–877, doi:10.1016/j.jpcs.2007.03.041 (2007).
  25. Akola, J., Larrucea, J. & Jones, R. O. Polymorphism in phase-change materials: melt-quenched and as-deposited amorphous structures in Ge<sub>2</sub>Sb<sub>2</sub>Te<sub>5</sub> from density functional calculations. *Phys. Rev. B* **83**, 094113 (2011).

## Acknowledgments

This research was supported by the “Convergence Technology Program” funded by KIST Institutional Program (Grant No. 2V03330). YGC acknowledges financial support from Basic Science Research Program of the National Research Foundation of Korea (NRF) funded by the Ministry of Education Science and Technology (2012R1A1A2003832).

## Author contributions

S.L. planned and managed the project. S.-Y.S. performed the experiments with the help of J.M.C., J.S. and H.-W.A. B.-k.C., Y.G.C. and S.L. took care of the data analyses and wrote the manuscript.

## Additional information

Supplementary information accompanies this paper at <http://www.nature.com/scientificreports>

**Competing financial interests:** The authors declare no competing financial interests.

**How to cite this article:** Shin, S.-Y. *et al.* The effect of doping Sb on the electronic structure and the device characteristics of Ovonic Threshold Switches based on Ge-Se. *Sci. Rep.* **4**, 7099; DOI:10.1038/srep07099 (2014).



This work is licensed under a Creative Commons Attribution-NonCommercial-NoDerivs 4.0 International License. The images or other third party material in this article are included in the article's Creative Commons license, unless indicated otherwise in the credit line; if the material is not included under the Creative Commons license, users will need to obtain permission from the license holder in order to reproduce the material. To view a copy of this license, visit <http://creativecommons.org/licenses/by-nc-nd/4.0/>